ELEVENTH INTERNATIONAL CONFERENCE ON INTERGRANULAR AND INTERPHASE BOUNDARIES 2004

JOURNAL OF MATERIALS SCIENCE **40** (2005) 3101 – 3106

TEM observation of gold nanoparticles deposited on cerium oxide

T. AKITA*
Research Institute for Ubiquitous Energy Devices, National Institute of Advanced Industrial Science and Technology (AIST), AIST Kansai, Midorigaoka 1-8-31, Ikeda, Osaka 563-8577, Japan
E-mail: t-akita@aist.go.jp

M. OKUMURA
Department of Chemistry, Graduate School of Science, Osaka Univ., Machikaneyama 1-1, Toyonaka, Osaka 560-0043, Japan

K. TANAKA, M. KOHYAMA
Research Institute for Ubiquitous Energy Devices, National Institute of Advanced Industrial Science and Technology (AIST), AIST Kansai, Midorigaoka 1-8-31, Ikeda, Osaka 563-8577, Japan

M. HARUTA
National Institute of Advanced Industrial Science and Technology, AIST Tsukuba, Umezono1-1-1, Tsukuba, Ibaraki 305-8568, Japan

The structure of Au nanoparticles supported on CeO_2 using the deposition precipitation method was observed using a transmission electron microscope (TEM). The shape of Au nanoparticles and the fine structure of contact interface between the Au nanoparticles and CeO_2 supports were carefully examined. It was found that there was a preferential orientation relationship between Au nanoparticles and the CeO_2 support. It was also observed that small and thin Au nanoparticles disappeared during TEM observation, shrinking layer by layer down to a mono-atomic layer.

1. Introduction

It has been reported that Au exhibits remarkably high catalytic activity when finely dispersed with particle diameters smaller than 10 nm on a selected metal oxide support [1]. The catalytic properties of Au nanoparticles are sensitive to the interface structure between the Au and metal oxide support. In particular, the structure of Au on TiO_2 was studied by various surface science techniques and theoretical calculations [2–5]. Other metal oxides can also be used for the support of Au catalysts, and the various combinations of Au particles and metal oxide supports are applicable to many kinds of catalytic reactions.

It was reported that Au/CeO_2 catalysts show high catalytic activity for low temperature water gas shift reaction and CO oxidation [6–8]. Au/CeO_2 catalysts prepared using the deposition precipitation method also showed high catalytic activity for the oxidative decomposition of volatile organic compounds [9]. Recently, it was reported that small clusters of atomically dispersed Au positively charged on a CeO_2 surface were responsible for low temperature water gas shift reaction [10]. However, the detailed structure of Au particles on CeO_2 was not investigated directly because it is difficult to observe small Au clusters on CeO_2 by conventional transmission electron microscopy (TEM) due to the disturbance of the diffraction and phase contrast by the CeO_2 substrate.

The structure of Au/CeO_2 catalysts was observed using an analytical transmission electron microscope in a previous work [11]. Annular dark field scanning transmission electron microscopy (ADF-STEM) and energy dispersive X-ray spectroscopy (EDS) revealed that Au particles smaller than 2 nm in diameter were highly dispersed on the CeO_2 support [11]. However, the CeO_2 support, which consisted of small crystals with a size of approximately 10 to 20 nm, disturbed detailed observations around the contact interface between Au and CeO_2.

In this work, TEM observations were performed on a model catalyst sample that was prepared using a CeO_2 support with a lower surface area and low index facets in order to study the interface structure between metal particles and CeO_2.

---

*Author to whom all correspondence should be addressed.

2. Experimental

Gold nanoparticles were deposited on commercially-produced, high-purity CeO_2 powder (Kojundo Chemicals Lab. Co., purity 99.99%) using the deposition precipitation method [12], which is utilized for the preparation of highly dispersed Au particles on metal oxide. The CeO_2 support was dispersed in a suitable volume of aqueous solution of $HAuCl_4$ at a fixed pH of 7. The Au content of the solution was 5.0 wt% with respect to the weight of the CeO_2 support. The dispersion was aged at 343 K for 1 h and washed with distilled water several times. The solid material was then vacuum dried at 0.4 Pa for 15 h at room temperature and calcined at 673 K in air for 4 h.

The Au/CeO_2 samples were dispersed directly on a carbon grid supported by a Cu mesh and no solvent such as ethanol was applied. A JEOL JEM-3000F transmission electron microscope was used with an accelerating voltage of 300 kV to study the Au/CeO_2 interface structure.

3. Results and discussion

Fig. 1 shows a typical TEM image of a Au/CeO_2 sample. The CeO_2 support consists of grains with diameters of approximately 50 to 100 nm and has low index facets typically in the {111} and {100} planes. Gold particles with diameters of 3 to 5 nm are deposited almost uniformly over the CeO_2 surface. Some Au particles are supported on the flat facets of CeO_2 as can be seen on the left side of the TEM image in Fig. 1. This enables us to investigate the interface structure. The Au particles in the center of the image are supported in a depression in the CeO_2 surface. Moiré fringes generated by the overlap of lattice fringes of Au particles and the CeO_2 support were sometimes observed as can be seen in the right side of the TEM image in Fig. 1.

Fig. 2a shows a plane view HRTEM image of Au on a CeO_2 support. An enlarged image of the Au nanoparticle indicated by the white rectangle is shown in Fig. 2b. The incident electron beam direction was parallel to the $\langle 110 \rangle$ zone axis of the cubic fluorite structure of the CeO_2. Moiré fringes in two directions were observed in the Au particles. The patterns of moiré fringes appeared in the same direction for each Au particle, indicating that the Au particles were deposited on the CeO_2 support with a preferred orientation relationship. The schematic drawing of a crystal model projected in Au$\langle 110 \rangle$ and $CeO_2\langle 110 \rangle$ directions is shown in Fig. 2c. The Au{111} plane is parallel to the CeO_2{111} plane and the $\langle 110 \rangle$ direction of Au and CeO_2 is also parallel. The lattice spacing is 0.235 and 0.312 nm for Au{111} and CeO_2{111}, respectively. The lattice mismatch is approximately 28%, which is too large for an epitaxial growth. However, the Au{111} spacing multiplied by four coincides with the CeO_2{111} spacing multiplied by three and is approximately 0.94 nm as indicated in Fig. 2c.

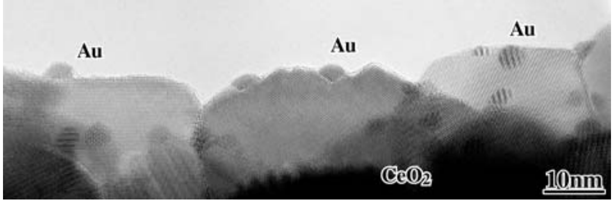

Figure 1 A typical TEM image of Au nanoparticles on a CeO_2 support.

Fig. 3 shows HRTEM images of Au nanoparticles deposited on CeO_2. The CeO_2 support has low index flat facets typically in the {111} and {100} planes. Au nanoparticles with diameters of approximately 3 nm are dispersed over the CeO_2{111} surface as can be seen in Fig. 3a and b. The orientation relationship between Au nanoparticles and the CeO_2 support is $(111)[1\bar{1}0]_{Au}//(111)[1\bar{1}0]_{CeO_2}$, which is the same as observed in Fig. 2. The orientation relationship of $(111)[1\bar{1}0]_{Au}//(111)[\bar{1}10]_{CeO_2}$ is also the same as that observed in Fig. 2b. The shape of the Au particles is a hemisphere, which means that the contact angle is small indicating a strong bonding between Au and CeO_2. It is noteworthy that the surface of the CeO_2 support is clean and flat, being free from the amorphous layer that is often observed on metal oxide surfaces such as TiO_2 [13]. Thus, it is likely that CeO_2 crystals are in direct contact with Au particles without any transition layers that have an obvious different crystal structure, such as corundum Ce_2O_3 with a different oxidation state. As previously mentioned, the hemispherical Au particle indicates that the Au strongly connected to the CeO_2 surface. Au atoms are most likely bonded to Ce atoms. It was reported that with Au on a TiO_2 surface, oxygen defects cause strong contact between the Au and TiO_2 surface and also effect a change in the electronic structure [5]. The local electronic structure is important as it affects catalytic properties. Further investigation is needed to determine the stoichiometry of the top layer of the CeO_2 support around the contact interface, because oxygen vacancies are easily created on a CeO_2surface [14]. The mean diameter of Au particles was approximately 4 nm and particles smaller than 2 nm diameter were seldom observed. In contrast, such small Au particles were observed on a CeO_2 support with a high specific surface area (>100 m^2/g) and that consisted of small CeO_2 crystal grains of approximately 10 to 30 nm diameter and many grain boundaries [11]. Such defects suppress the growth of Au particles, so the size distribution of Au is dependant on the surface morphology of the support. Disordered atoms can be seen on the right side of the Au particles in Fig. 3a and b. The atoms might be reconstructed surface Au atoms, or Ce atoms coming from the substrate as reported of Rh/CeO_2 or Pt/CeO_2 catalysts [15]. The composition of the disordered layer was not analyzed in the present study. A lattice fringe different from the bulk region appears on the surface of the CeO_2 around Au particles. Because the lattice space is same as the lattice space of the bulk region of CeO_2, this contrast may be due to difference in the thickness of CeO_2 support, such as an atomic-layer island of CeO_2. It is feasible that Au particles tend to be supported on such defect sites.

Fig. 4 shows a series of HRTEM images of Au particles on a $CeO_2(111)$ surface obtained during TEM observation. Each successive HRTEM image was taken

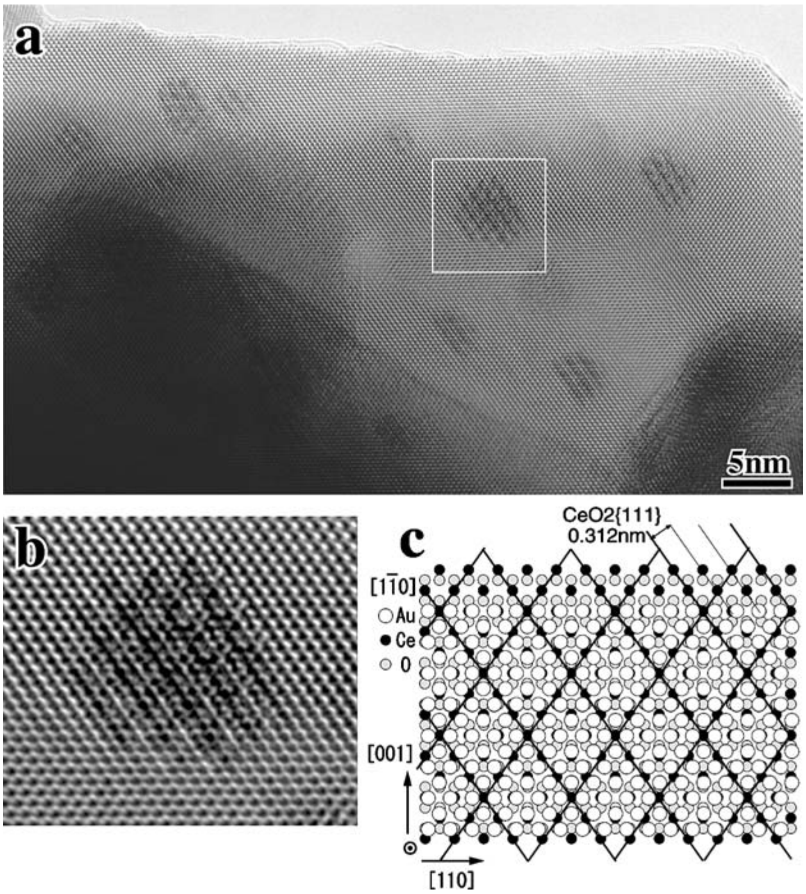

Figure 2 (a) TEM images of Au particles on a CeO_2 support, (b) enlarged image of the region marked by the white rectangle, and (c) schematic drawing of the crystalline orientation between Au and CeO_2.

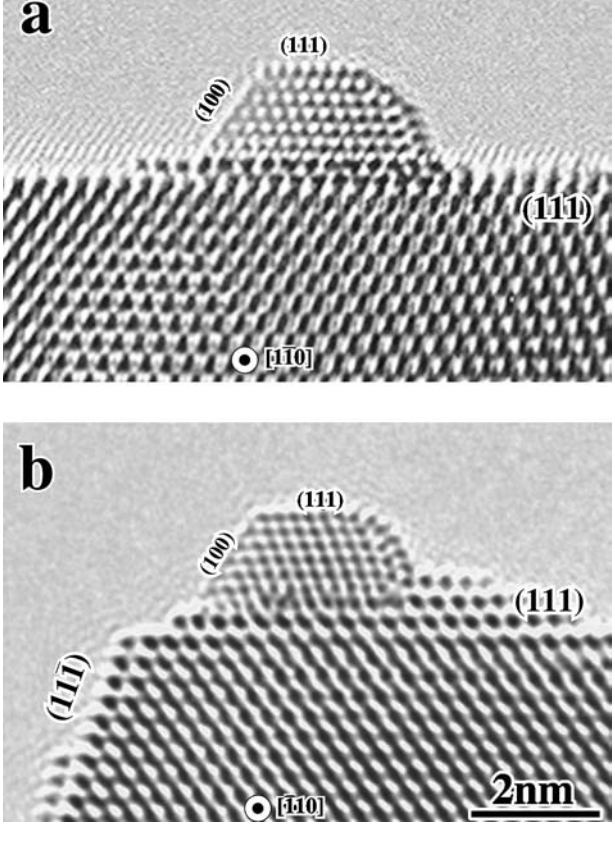

Figure 3 HRTEM image of Au particles supported on $CeO_2(111)$ facets.

after a further few minutes of illumination by the electron beam. A large Au particle can be seen on the left side of these images supported at the step edge of the $CeO_2(111)$ surface. A smaller Au particle can be seen in the right side of some images, also supported at the edge of an atomic step. The orientation relationship is $(111)[1\bar{1}0]_{Au}//(111)[1\bar{1}0]_{CeO_2}$ as was also observed in Figs 2 and 3a. The smaller Au particle disappeared during observation while the larger Au particle remained. This change is similar to Ostwald ripening and the transport of atoms may occur by surface diffusion along the CeO_2 surface. No apparent volume change could be detected in the larger Au particle. Even if all the atoms in the small particle were added to the large particle, the increment in diameter of the large particle would only be 0.06 nm, which is smaller than one atomic layer. It is difficult to determine such a small change in particle size in three dimensions from a TEM image.

The height of the smaller Au particle decreased layer by layer, while the length of contact interface (indicated by the white line) remained unchanged until the thickness was reduced to one atomic layer. This means that the Au atoms at the contact interface are strongly connected to the CeO_2 surface. It seems that equilibrium Au clusters of two-shell Au55 or one-shell Au13 clusters [16] cannot be formed on the CeO_2 surface, because Au particles grow on the CeO_2 surface by atomic layer at the initial stage, as was proposed for Au on a TiO_2 surface [17]. It seems that the interface energy between

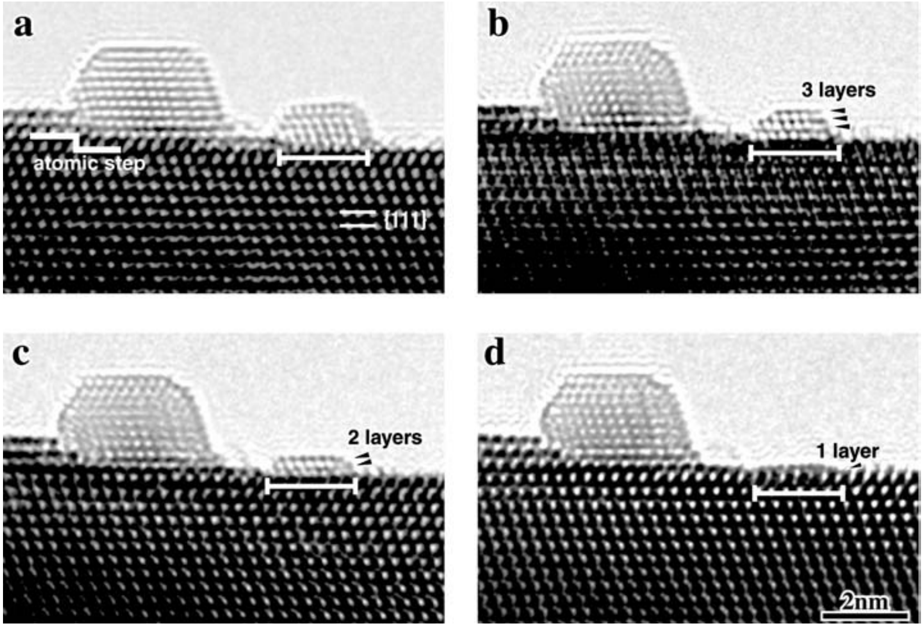

Figure 4 A series of HRTEM images revealing the shrinking process of an Au particle on a $CeO_2(111)$ facet.

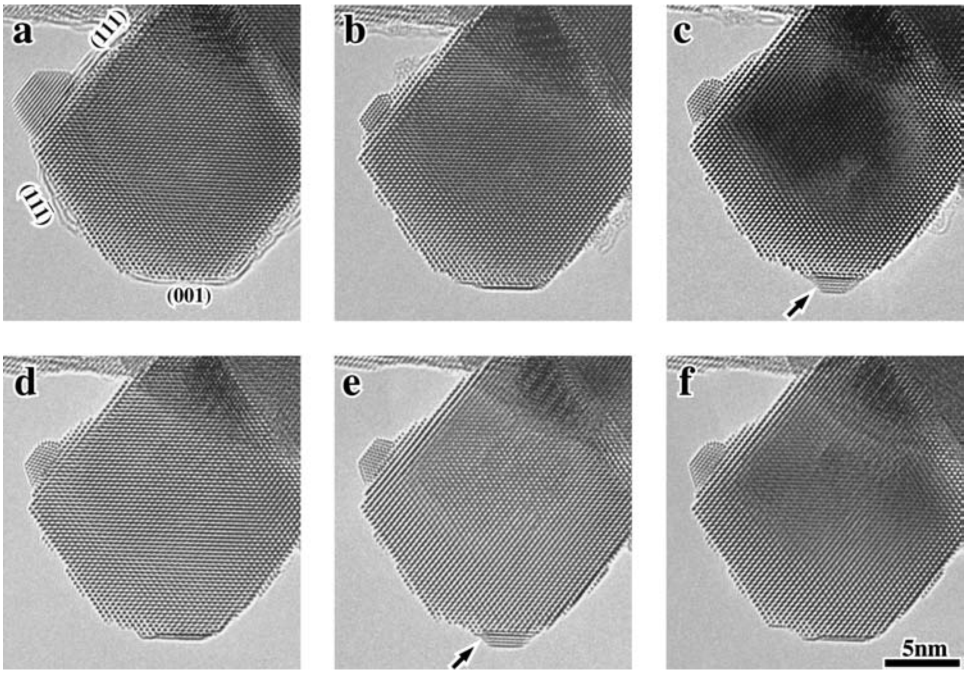

Figure 5 A series of HRTEM images showing the diffusion process of Au particles on CeO_2.

Au and CeO_2 is so small that Au atoms tend to form a film structure rather than spherical clusters.

Fig. 5 shows a series of TEM images of Au particles on a CeO_2 support during TEM observation. Both (111) and (100) facets were observed on the CeO_2 support. As can be seen in Fig. 5a, only one Au particle was observed on $CeO_2(111)$ at the initial stage of observation. The Au particle became smaller during observation as can be seen in Fig. 5b. A second Au particle appeared on the $CeO_2(100)$ facet after leaving the sample for 5 to 10 min without electron beam irradiation. The orientation relationship between the Au particle and the CeO_2 support is Au(111)//$CeO_2(100)$. The appearance and disappearance of the Au particle was reversible. During observation, the Au particle on the (100) surface gradually became smaller as did the Au particle on the (111) surface, as can be seen in Fig. 5b, d and f. After each observation, the electron beam was turned off and the sample was left for 5 to 10 min in this condition before turning the electron beam on again. The Au particle observed on the (100) surface can be seen in Fig. 5c and e.

The crystal structure of the CeO_2 support was stable during observation over 10 to 20 min, whereas other metal oxides such as TiO_2 crystal are easily destroyed by electron beam irradiation. It can be confirmed by electron energy loss spectroscopy (EELS) measurement that the CeO_2 support is also reduced by electron irradiation, even though structural change in the crystal was not observed in TEM images.

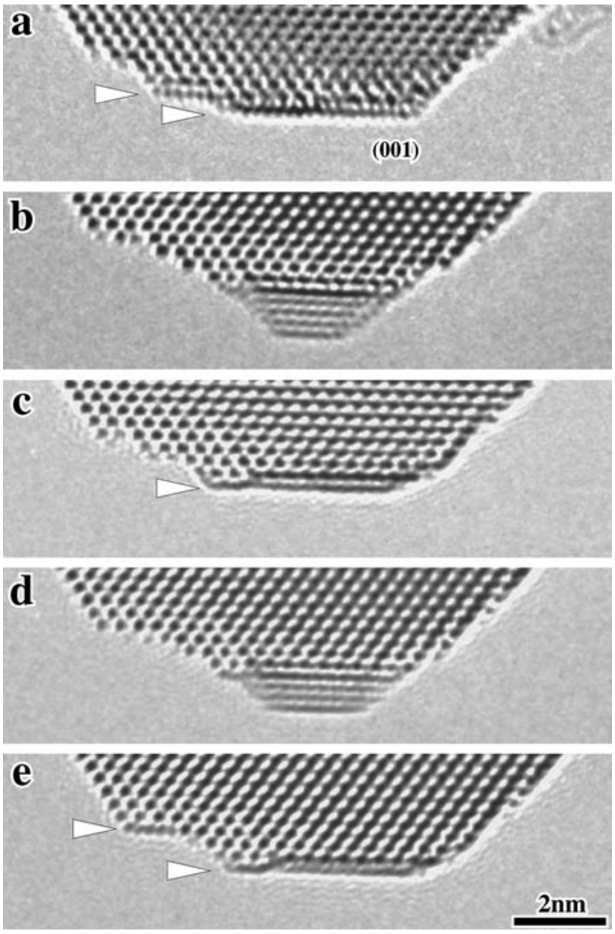

Figure 6 A series of HRTEM images revealing the diffusion process that leads to the growth of an Au particle on $CeO_2(100)$.

Fig. 6 shows enlargements of the HRTEM images in Fig. 5 centered around the $CeO_2(100)$ surface. The Au particle also shrunk layer by layer. When the Au particle was shrinking, an atomic layer was observed around the (001) face as shown by white arrow heads in Fig. 6a, c and e. It is probable that Au atoms diffused onto the CeO_2 surface during the shrinking process of the Au particle. Although it has been determined that Au or Pt atoms can diffuse into bulk CeO_2 crystal depending on the temperature and atmosphere [18, 19], it was not confirmed in this HRTEM observation whether the Au atoms did diffuse into the bulk.

Fig. 7 shows a schematic drawing of the diffusion process of Au particles on the CeO_2 surface. Many Au atoms are diffused onto the CeO_2 surface by the irradiation of the electron beam. When the electron beam is turned off, Au nuclei are formed on the $CeO_2(100)$ surface and the Au particles grow. The volume of Au was approximately estimated from the TEM images assuming that the Au particles have a hemispherical shape. The initial volume of the Au particle indicated in Fig. 5a was 22 nm^3, and that of the Au on $CeO_2(111)$ and Au on $CeO_2(100)$ in Fig. 5c was 7 nm^3 and 4 nm^3, respectively. This means that many Au atoms are still diffusing onto the CeO_2 surface in Fig 5c and e. It seems that the temperature rise caused by electron beam irradiation is the driving force for the diffusion of Au atoms. However, it is difficult to estimate the precise temperature of an Au particle. It seems that the temperature of Au nanoparticles under TEM observation is significantly lower than the melting point of bulk Au (1336 K), considering that the temperature of the Au particles on MgO under TEM observation is estimated at below 373 K [20]. However, the melting point of metals depends on particle size, and the melting point of a Au particle with a size of approximately 2 nm diameter is estimated to be below 573 K [21]. Thus, the electron beam irradiation may cause sufficient driving force for atomic transfer in the small Au particles. Another possibility is that a change in the surface structure of CeO_2, such as oxygen defects created by the electron irradiation, promotes the diffusion of Au atoms. It was proved in an earlier study that the diffusion of Au on metal oxides is strongly affected by oxygen surface defects [22]. Further investigation will reveal the details of the diffusion process of Au on CeO_2.

4. Conclusions

The following conclusions were drawn following a TEM study of Au particles supported on CeO_2 using the deposition precipitation method.

(1) Gold particles are supported on CeO_2 as hemispherical nanoparticles with the preferential orientation relationship: $(111)[1\bar{1}0]_{Au}//(111)[1\bar{1}0]_{CeO_2}$ and $(111)[1\bar{1}0]_{Au}//\ (111)[\bar{1}10]_{CeO_2}$.

(2) The hemispherical Au particles are strongly supported by the CeO_2 support having sufficiently long perimeter interfaces between Au and CeO_2.

(3) Smaller Au particles easily diffuse onto the CeO_2 surface by atomic transport.

Acknowledgement

Part of this work was supported by the Japan Society for the Promotion of Science (JSPS-Grant-in-Aid for Scientific Research (B)). The authors are grateful to Drs. S. Ichikawa, K. Okazaki, and S. Tanaka for their valuable comments and stimulating discussion.

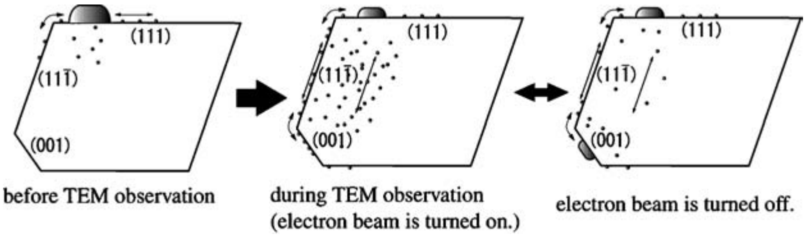

Figure 7 Schematic drawing of the possible diffusion process of Au onto the CeO_2 surface.

References

1. M. HARUTA, *Catal. Today* **36** (1997) 153.
2. M. VALDEN, X. LAI and D. W. GOODMAN, *Science* **281** (1998) 1647.
3. Y. MAEDA, M. OKUMURA, S. TSUBOTA, M. KOHYAMA and M. HARUTA, *Appl. Surf. Sci.* **222** (2004) 409.
4. N. LOPEZ and J. K. NØRSKOV, *ibid.* **515** (2002) 175.
5. K. OKAZAKI, Y. MORIKAWA, S. TANAKA, K. TANAKA and M. KOHYAMA, *Phys. Rev. B* **69** (2004) 235404.
6. Q. FU, A. WEBER and M. FLYTZANI-STEPHANOPOULOS, *Catal. Lett.* **77** (2001) 87.
7. H. SAKURAI, S. TSUBOTA and M. HARUTA, *Catalyst & Catalysis* **44** (2002) 416.
8. S. CARRETTIN, P. CONCEPCIÒN, A. CORMA, J. M. L. NIETO and VICTOR F. PUNTES, *Angew. Chem. Int. Ed.* **43** (2004) 2538.
9. S. SCIRÈ, S. MINICÒ, C. CRISAFULLI, C. SATRIANO and A. PISTONE, *Appl. Catal. B: Environm.* **40** (2003) 43.
10. Q. FU and M. FLYTZANI-STEPHANOPOULOS, *Science* **301** (2003) 935.
11. T. AKITA, M. OKUMURA, K. TANAKA, M. KOHYAMA, S. TSUBOTA and M. HARUTA, in Proceedings of 8th Asia-Pacific Conference on Electron Microscopy (2004) p. 644.
12. S. TSUBOTA, D. A. H. CUNNINGHAM, Y. BANDO and M. HARUTA, in “Preparation of Catalysts IV”, edited by G. Poncelt, J. Martens, B. Delmon, P. A. Jacobs and P. Grange (Elsevier, Amsterdam,1995) p. 227.
13. T. AKITA, K. TANAKA, S. TSUBOTA and M. HARUTA, *J. Electron Microsc.* **49** (2000) 657.
14. A. TROVARELLI, in “Catalysis by Ceria and Related Materials”, edited by A. Trovarelli (Imperial College Press, London, 2002) p. 15.
15. S. BERNAL, J. J. CALVINO, M. A. CAUQUI, J. M. GATICA, C. LARESE, J. A. PÈREZ OMIL and J. M. PINTADO, *Catal. Today* **50** (1999) 175.
16. F. COSANDEY and T. E. MADEY, *Surf. Rev. Lett.* **8** (2001) 73.
17. A. L. MACKAY, *Acta Cryst.* **15** (1962) 916.
18. P. BERA and M. S. HEGDE, *Catal. Lett.* **79** (2002) 75.
19. P. BERA, K. R. PRIOLKAR, A. GAYEN, P. R. SARODE, M. S. HEGDE, S. EMURA, R. KUMASHIRO, V. JAYARAM and G. N. SUBBANNA, *Chem. Mater.* **15** (2003) 2049.
20. S. IIJIMA and T. ICHIHASHI, *Phys. Rev. Lett.* **56** (1986) 616.
21. PH. BUFFAT and J.-P. BOREL, *Phys. Rev. A* **13** (1976) 2287.
22. Y. MAEDA, T. FUJITANI, S. TSUBOTA and M. HARUTA, *Surf. Sci.* **562** (2004) 1.

Received 9 September 2004
and accepted 31 January 2005